A preliminary design procedure for optimizing insulated structures of hypersonic flight vehicles is described. It is useful for selecting and sizing both insulating and structural materials to minimize weight or volume. Studies based on this method show that weight penalties resulting from insulation thicknesses greater than optimum are smaller than those resulting from less-than-optimum thicknesses. It is concluded that lightly loaded, insulated structures can be operated at higher temperatures than have heretofore been considered as efficient for the material.

R. M. Rivello

A DESIGN METHOD FOR OPTIMIZING insulated structures FOR HYPERSONIC VEHICLES

The aerodynamic heating that occurs in high-velocity flight vehicles greatly influences their structural design. The high temperatures that result can have a serious effect on the strength and stiffness of the structural materials. In addition, large thermal gradients generated during high-speed flight can cause thermal stresses that result in failure of the structural materials.

In hypersonic flight the surface temperature range of air-breathing vehicles is predicted to be from 2000 to 6000°F. While unprotected "super-alloy" metal structures have been used for supersonic vehicles, more sophisticated designs are generally required for the hypersonic-vehicle temperature range. Refractory metals can endure short-time operation in the lower portion of this range, but because they exhibit low strength and stiffness at these temperatures their use may result in excessive weight penalties. None of the refractory metals can withstand the high temperatures that may occur in the propulsion system and on the leading edges of hypersonic vehicles.

Apparently, thermal protection of major portions of hypersonic vehicles will be necessary to achieve acceptable airframe weights. There are three basic means of achieving this protection: active thermal protection (coolants); passive thermal protection (ablators); and insulator systems. The latter are of concern in the present paper because they have two distinct advantages that make them of interest in solving structural problems of hypersonic flight vehicles; comparatively stable geometry and relative ease of analysis.

The choice of materials for an insulator system is usually made on the basis of comparative costs, reliability, and structural efficiency. The relative structural efficiency of materials for the vehicle is judged on the basis of lowest weight, or, if space is critical, the least volume possible for a given thermal environment and load.

In other papers on this subject[1,2,3] the thermal capacity of the insulating layer has been assumed to be negligible. The work to be described in this article[4] was undertaken as an extension of the investigations of Davidson[1] and of Davidson and Dolby,[2] to include the insulation's thermal capacity and also to consider higher surface temperatures and specific combinations of insulating and structural materials. Our investigation was limited to structures protected by a single insulating layer.

[1] J. R. Davidson, *Optimum Design of Tension Members Subjected to Aerodynamic Heating,* NASA TN D-117, 1959.

[2] J. R. Davidson and J. F. Dolby, *Optimum Design of Insulated Compression Plates Subjected to Aerodynamic Heating,* NASA TN D-520, 1961.

[3] R. S. Harris, Jr. and J. R. Davidson, *Methods for Determining the Optimum Design of Structures Protected from Aerodynamic Heating and Application to Typical Boost-Glide or Re-entry Flight Paths,* NASA TN D-990, 1962.

[4] For a complete description of this work see: R. M. Rivello, *Preliminary Design Methods for the Optimization of Insulated Structures for Hypersonic Cruise Vehicles,* CF-3085, The Johns Hopkins University, Applied Physics Laboratory, May 15, 1964.

Method of Analysis

A sketch of a typical section from an insulated structure is shown in Fig. 1. The interlocking tile scheme shown was adopted to avoid large thermal stresses in the structure, which would result if a continuous insulating layer were bonded to the metal structure. Thermal stresses are neglected in the metal, and the segmented insulation is free to expand. Use of a segmented insulation layer results in the total applied load being borne by the metal structure. As can be seen in Fig. 1, both the insulation and structural material can be characterized by their specific weight, ω, thermal conductivity, k, and specific heat, c. The adiabatic wall temperature, T_{aw}, and the heat transfer coefficient, h, at the surface of the insulation are generally functions of time. The temperature of the metal structure, starting from an initial value T_0, reaches a value T_2 after exposure to the air flow for a given time, τ.

For a given thermal environment and exposure time, the weight of the structural layer increases with T_2 as a result of the thermal degradation of its mechanical properties. On the other hand, the required weight of the insulation decreases as T_2 increases. These trends are shown in Fig. 2. As would be expected the total weight of the structure reaches a minimum optimum weight at one particular design structural temperature. This is precisely the information the missile designer needs to insure structural efficiency.

An exact solution of the structural efficiency problem is not justified for a preliminary design, as the thermal environment and loads are seldom known with sufficient accuracy for elaborate solutions. It appears desirable, therefore, to introduce simplifying assumptions so that an approximate solution can be found. These are:

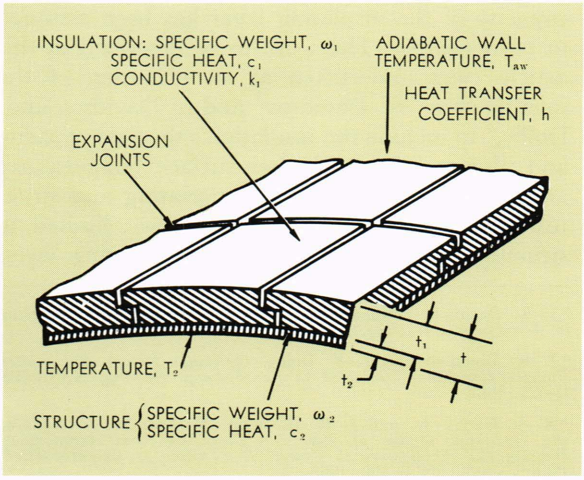

Fig. 1—Cross section of a typical insulated flight structure.

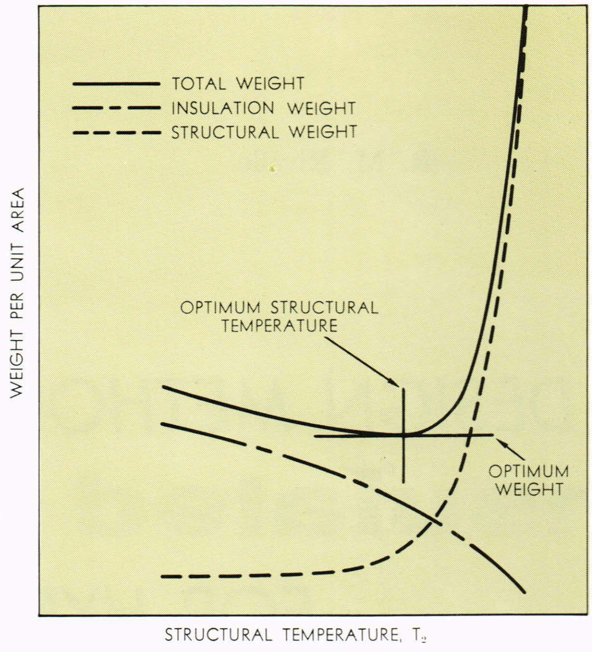

Fig. 2—Variation of weight per unit surface area with structural temperature.

1. *The heat flow is one-dimensional in the direction normal to the surface.* This assumption is justified except in the regions of leading edges and shock or expansion wave impingements where large thermal gradients may occur in the plane of the surface.

2. *The thermal resistance at the interface of the insulator and the metal structure may be neglected.*

3. *Following an initial step change at time zero, the quantities* T_{aw} *and* h *do not vary during time of exposure,* τ. This assumption limits the missile design to certain types of vehicles and trajectories. It has been found to be sufficiently accurate for the preliminary design of ramjet missiles, which usually accelerate rapidly to a nearly constant cruise Mach number and altitude. The assumption would probably not be true for the case of ballistic-trajectory re-entry vehicles.

4. *The temperature is constant through the thickness of the metal.* This assumption can be made if the thermal conductivity of the structural metal is large relative to that of the insulator and if its thickness is comparatively small. It is equiva-

lent to assuming that the structural metal has an infinite coefficient of conductivity.

5. *The thermal properties of the materials are independent of the local temperature and therefore do not vary through the thickness of the insulator.* The large temperature changes associated with hypersonic flight strain the validity of this assumption. To alleviate this in part, the conductivity and specific heat of the insulation can be taken as their integrated mean values over the range of temperatures from the initial temperature, T_0, to the final value of the wall temperature, T_2; and the specific heat of the structural material can be taken as its integrated mean value over the temperature interval from T_0 to T_2.

6. *No heat is lost from the back face of the structure.* This is equivalent to assuming that the back face of the structure acts as a perfectly insulated surface. This assumption is conservative, especially for cases in which the structural material is in contact with fuel; the fuel will function as a large heat sink.

Design Procedure

To illustrate the optimization procedure we consider an insulated unstiffened shell structure with a circular cross section of radius, R, which is subjected to a bursting pressure, p. The dimension R is assumed fixed by other design considerations. The ratio of R to the thickness of the shell, t, is assumed sufficiently large to allow the use of the plate solution for heat transfer. The objective of this design method, it should be recalled, is to select materials and thicknesses that minimize either the weight or the thickness of the composite structure for a given thermal and load environment.

As suggested by Grover and Holter,[5] two dimensionless variables are chosen:

$$Y = \frac{T_{aw} - T_2}{T_{aw} - T_0}, \tag{1}$$

and

$$X = \frac{k_1 \tau}{\omega_1 c_1 t_1^2}. \tag{2}$$

It can be determined from a plot of Y and X (Fig. 3) that for Y less than 0.9 and X greater than 0.5 the curves of $\ln Y$ versus X are essentially linear. Further, if these linear segments are extended, they appear to converge at a point, and their slopes are very nearly inversely proportional to a linear function of the parameter μ, defined by

$$\mu = \frac{k_1}{ht_1} + \frac{c_2\omega_2 t_2}{c_1\omega_1 t_1} + \left(\frac{k_1}{ht_1}\right)\left(\frac{c_2\omega_2 t_2}{c_1\omega_1 t_1}\right). \tag{3}$$

These lines, then, may be approximated by

$$\ln Y = a + bX, \tag{4}$$

where the slope, b, of the lines is a function of μ and a is the intercept of the straight lines. The previously-referred-to point of convergence of the linear approximations to the lines of constant μ has the coordinates $X = 0.1$ and $Y = 1.0$. Substituting these coordinates into Eq. 4 gives $a = -0.1b$.

Using the fact that the slopes of the lines are nearly inversely proportional to a linear function of μ, Eq. 4 can be rewritten as

$$\ln Y = \frac{X - 0.1}{c + d\mu}. \tag{5}$$

The constants c and d can be found by matching two of the line segments of Fig. 3 to Eq. 5. The lines chosen in this case were $\mu = 0.0$ and $\mu = 1.6$ (the latter value was chosen because it falls in the

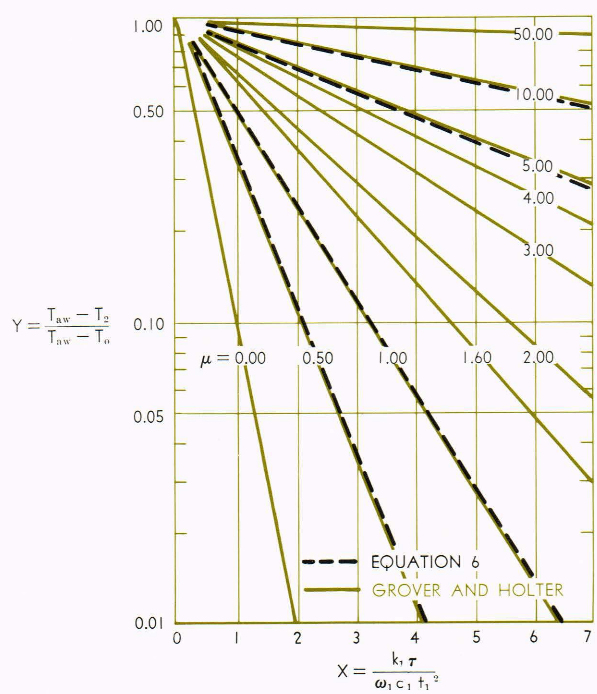

Fig. 3—Dimensionless plot of temperature rise versus heating time (Ref. 5).

[5] J. H. Grover and W. H. Holter, "Solution of the Transient Heat-Conduction Equation for an Insulated, Infinite Metal Slab," *Jet Propulsion,* **27**, Dec. 1957.

middle range of the curves), which gives

$$\ln Y = -\frac{4.605\,(X - 0.1)}{1.87 + 4.52\mu}\,. \tag{6}$$

The results of using Eq. 6 are shown by the dashed lines in Fig. 3. With the values of μ and X, as expressed in Eqs. 2 and 3, Eq. 6 can be solved for the thickness of the insulator, t_1:

$$t_1 = -\frac{2.26\left(\frac{k_1}{h} + \frac{\omega_2 c_2 t_2}{\omega_1 c_1}\right)\ln Y}{(1.87\ \ln Y - 0.4605)} + \left\{\left[\frac{2.26\left(\frac{k_1}{h} + \frac{\omega_2 c_2 t_2}{\omega_1 c_1}\right)\ln Y}{(1.87\ \ln Y - 0.4605)}\right]^2 - \left[\frac{4.605\,\frac{k_1\tau}{\omega_1 c_1} + 4.52\,\frac{k_1\omega_2 c_2 t_2}{h\omega_1 c_1}\ln Y}{(1.87\ \ln Y - 0.4605)}\right]\right\}^{\frac{1}{2}}. \tag{7}$$

The values of t_1 from this equation are not as accurate as those that can be found by directly interpolating Fig. 3. However, since they are found from an analytic expression they are much more convenient for preliminary design purposes. In hypersonic vehicles the heat transfer coefficients are large, and if an efficient insulator is used, k_1 is small enough so that the terms containing k_1/h may be neglected. If this is done, Eq. 7 simplifies to

$$t_1 = -\frac{2.26\,\frac{\omega_2 c_2 t_2}{\omega_1 c_1}\ln Y}{(1.87\ \ln Y - 0.4605)} + \left\{\left[\frac{2.26\,\frac{\omega_2 c_2 t_2}{\omega_1 c_1}\ln Y}{(1.87\ \ln Y - 0.4605)}\right]^2 - \left[\frac{4.605\,\frac{k_1\tau}{\omega_1 c_1}}{(1.87\ \ln Y - 0.4605)}\right]\right\}^{\frac{1}{2}}. \tag{8}$$

This simplification is equivalent to assuming that the temperature of the outer surface of the insulation undergoes a step change from T_0 to T_{aw} at time zero and is constant thereafter.

If the cylinder is long, so that end restraint effects are unimportant, the hoop stress is given by

$$\sigma = \frac{pR}{t_2}\,. \tag{9}$$

This equation can be made more meaningful by substituting a limiting criterion for σ. The maximum tensile stress, σ_{tu}, is a function of the temperature of the structural material and of τ. This function can be obtained from experimentation and used in Eq. 9. Ideally, the tensile loading history for such experiments should coincide with that of the pressure variations in the structure. With $\sigma_{tu}(T_2, \tau)$ in hand, the thickness of the metal structure can be determined, since p, the cylinder's bursting pressure, and R are known.

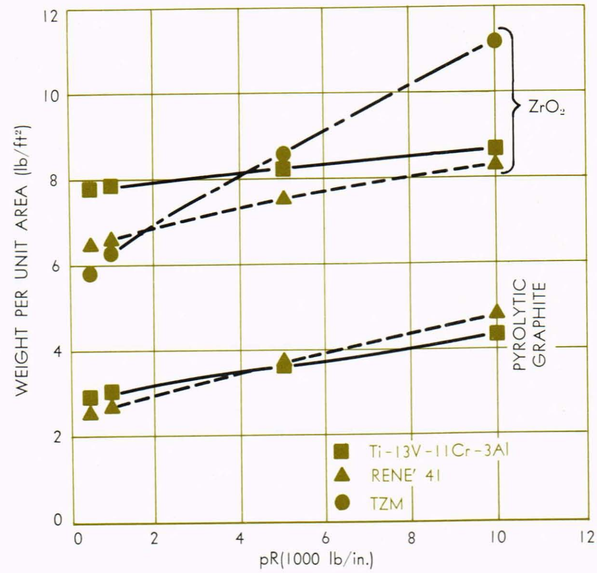

Fig. 4—Typical curves of optimum weight per unit area versus loading parameter, pR, for a pressurized cylinder, with T_{eq} = 4000° F and τ = 25 sec.

It is now possible to determine the thickness of the insulator and the metal structure for a given T_2 and p. The total thickness of the insulation and structure is

$$t = t_1 + t_2, \tag{10}$$

and the total weight per unit area, W, is

$$W = \omega_1 t_1 + \omega_2 t_2. \tag{11}$$

Curves such as the one shown in Fig. 2 may now be drawn. Further, by plotting pR against the optimum design weight determined from curves similar to those in Fig. 2, plots such as those shown in Fig. 4 can be drawn. With these it is possible to determine the optimum materials for the vehicle.

Curves of the above type, while they are very useful, can only be used for material selections when the insulated structure is subjected to a single design condition. A plot that displays more information and is also applicable to missiles with more than one design condition is shown in Fig. 5. This plot shows the data t_1, t_2, T_2, W, and t in a single figure. Fabrication and handling limitations imposed by the material thicknesses, or restrictions on T_2 imposed by the allowable bond temperature, can also be shown as design boundaries in this type of figure.

In constructing plots similar to Fig. 5, the dotted lines with T_2 as a parameter are drawn first. For a given thermal environment, this is done by successively fixing T_2 and using Eq. 7 or 8 to find t_1 for enough values of t_2 to establish a curve. Once the family of dotted lines is determined, the solid curve is found by successively fixing pR and overplotting the values of t_2 obtained from Eq. 9 on each of the T_2 curves. The lines of constant thickness and weight that are shown are obtained respectively from Eqs. 10 and 11. The curves may be used to obtain the design for a minimum weight or a minimum thickness, as shown by the points A and B, respectively.

This method of analysis may be used for other types of structures and loadings.[4] If this is done, however, Eq. 9 has to be generalized for other than the bursting pressure case. In general, for a given τ, t_2 can be written as

$$t_2 = \frac{\beta}{\gamma(T_2)} \cdot \qquad (12)$$

Expressions for β and γ for additional commonly encountered structural problems are given in Table I. The parameter γ contains the mechanical properties pertinent to the failure or limiting deflection criteria, and β is a function of the applied loading and the geometric dimensions.

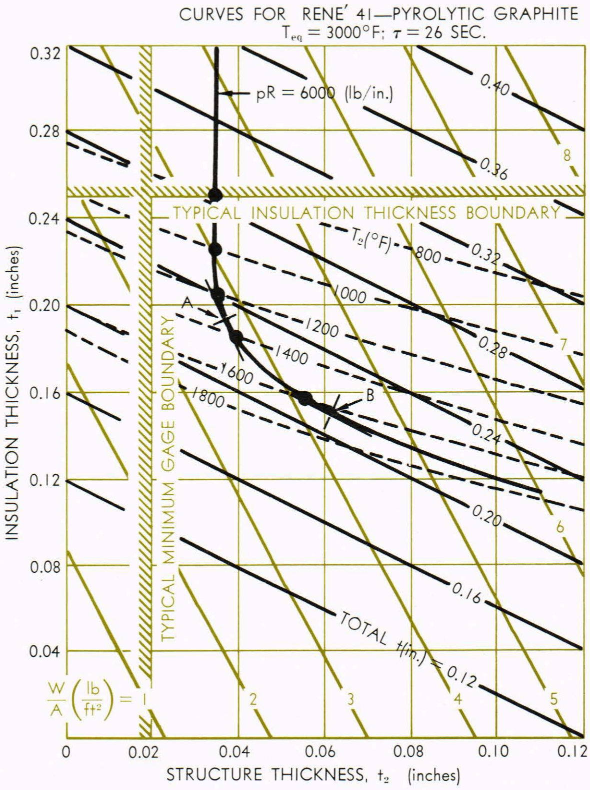

Fig. 5—Typical single-condition design curves for insulated flight structures.

Since flight vehicles must be capable of operating over a wide range of loading and thermal environments, the designer must find the optimum configuration for the combination of these environments. This can be accomplished by an extension of the information found in Fig. 5. Instead of plotting one constant pR curve, a separate curve for every set of environmental parameters is plotted. The area to the right and above any one of these curves constitutes the permissible values of thicknesses for the conditions to which it applies. The curves, then, when plotted for all the critical environments, will form an envelope of acceptable values for the weights and thicknesses. The optimum values can be found graphically as before. The weights and thicknesses obtained for one set of materials may be compared with those obtained for other materials to find the most efficient combination of insulator and metal structure.

Material Screening

The materials to be analyzed can often be limited by means of a material screening. As a rule of thumb, minimum weight is associated with structural metals that have minimum values of ω_2/γ and maximum values of c_2. Haynes René 41, TZM molybdenum alloy, Ti-13V-11Cr-3A1 titanium alloy, cross-rolled beryllium sheet, and HM21A-T81 magnesium alloy were selected on this basis for further study. The first four of these five materials are useful in tensile applications, and the last four in situations where buckling is critical. For minimum thickness the structural material should have large values of γ and $\omega_2 c_2$. A study of Eq. 7 shows that minimum-thickness insulations having large values of $\omega_1 c_1$ and small values of k_1 should be used. By multiplying Eq. 7 by ω_1, it is seen that for minimum weight large c_1 and small $k_1\omega_1$ are desirable. For long flight times the insulation thickness and weight become proportional to the square roots of the thermal diffusivity, $k_1\omega_1 c_1$, and the parameter $k_1\omega_1/c_1$, respectively. From these considerations pyrolytic graphite and zirconium dioxide appear to offer the most hope for lightweight insulated structures in the hypersonic regime. The conductivity and density of zirconium dioxide decrease with an increase in porosity so that its efficiency as an insulator is increased. Results in the remainder of this article are based upon a 25% porosity for the zirconium dioxide, which is felt to represent the most porous zirconium dioxide that could withstand the erosive action of hypersonic flow.

TABLE I

LOAD-GEOMETRY AND MECHANICAL PROPERTY PARAMETERS FOR VARIOUS STRUCTURES

Type of Structure	*Loading*	*Design Criteria*	*Dimensions*	*Load-Geometry Parameter* β	*Mechanical Property Parameter* γ	*Remarks*
I. Thin-walled circular cylinder	a. Radial bursting pressure	1. Material rupture		pR	σ_{tu}.	For high temperatures and steady load use creep rupture stress for given lifetime in place of σ_{tu}
		2. Limiting radial displacement	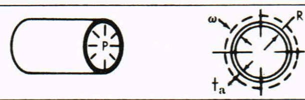	pR	Stress to give total % deformation $w_{allow.}/R$ at given lifetime.	Total % deformation includes elastic, plastic, and creep strain.
	b. Radial collapsing pressure	Buckling	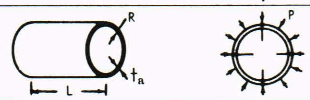	$\left(\frac{pR^{3/2}/L}{0.93}\right)^{2/5}$	$E^{2/5}$	$100\frac{t_2}{R} < \left(\frac{L}{R}\right)^2 < 5\frac{R}{t_2}$.
	c. Axial compression	Buckling	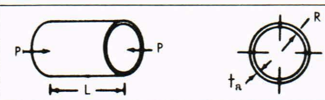	$\left(\frac{P}{2\pi C_c}\right)^{1/2}$	$E^{1/2}$	$C_c \approx 0.3$ for $L^2/Rt_2 > 100$.
	d. Bending	Buckling	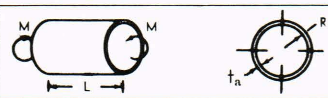	$\left(\frac{M}{\pi R C_b}\right)^{1/2}$	$E^{1/2}$	$C_b \approx 0.39$ for $L^2/Rt_2 > 100$.
II. Flat plate	a. Tension	Material rupture	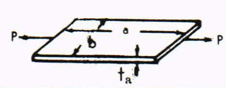	$\frac{P}{b}$	σ_{tu}	For high temperature and steady load use creep rupture stress for given lifetime in place of σ_{tu}.
	b. Compression	Buckling	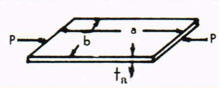	$\left(\frac{Pb}{K_c}\right)^{1/3}$	$E^{1/3}$	$K_c \approx 3.62$ for $a/b > 2$ and simply supported edges.

Results and Discussion

Investigations were carried out for the structural configurations and loadings described in Cases Ia, Ic, Id, and IIb of Table I, using combinations of structural materials and insulators chosen by the preliminary screening. The lightest structure in all of the cases investigated resulted from the use of pyrolytic graphite and beryllium. This is unfortunate since it combines the two most expensive materials, both of which have development problems. For a given metal the pyrolytic graphite insulation always results in a lighter design than the zirconium dioxide. For times τ between 20 and 60 sec, and insulator temperatures of 3000, 4000, and 5000°F, the preference of structural materials in descending order of weight efficiency is beryllium, Ti-13V-11Cr-3A1, René 41, HM21A-T81, and TZM, for medium to high values of loading parameter β in Case Ia (tensile loading). For medium to high values of the loading parameter in Cases Ic, Id, and IIb (buckling loading), the descending order of preference is beryllium, HM21A-T81, Ti-13V-11Cr-3A1, René 41, and TZM. The light materials (beryllium and HM21A-T81) used with zirconium dioxide are more efficient in buckling applications than are the dense materials used with pyrolytic graphite. It should again be pointed out that the results are for unstiffened shell structures. It is likely that the higher density materials, Ti-13V-11Cr-3A1, René 41, and TZM would be competitive or even more efficient if stiffened or if sandwich structures were used in the cases where failure occurs by buckling. The high-temperature, high-density, low-strength materials such as TZM do not appear efficient except at low-load levels. However, at 3000°F and low-load levels, uninsulated TZM appears to provide the most desirable design.

An examination of Fig. 2 and similar curves discloses some interesting facts. We see that it is more efficient to over-insulate than to under-insulate since the weight increases only slightly for temperatures below the optimum, but increases rapidly for temperatures above the optimum point. As would be expected, similar curves also show that as the load level increases the optimum structural temperature decreases. At low-load levels the optimum weight is reached at structural temperatures that are higher than those for which mechanical properties are well established. We have concluded, therefore, that lightly loaded, insulated structures can be operated at higher temperatures than have heretofore been considered within the efficient capability of the material.